STRUCTURE AND ELECTRON DENSITY IN $Ba_8Zn_xGe_{46-x}[\ ]_y$

E. Alleno[1], G. Maillet[1], O. Rouleau[1], E. Leroy[1], W. Carrillo-Cabrera[2], P. Simon[2], C. Godart[1], Yu. Grin[2]
1- ICMPE- CMTR, CNRS-UMR 7182, 2-8, rue H. Dunant, 94320 THIAIS, FRANCE
2- Max Planck Institute for Chemical Physics of Solids, Nöhnitzer Strasse 40, D-01187 DRESDEN, GERMANY
Contact author: eric.alleno@icmpe.cnrs.fr

Abstract

The superstructure we recently reported in the $Ba_8Zn_xGe_{46-x-y}[\ ]_y$ compounds ($4 \leq x \leq 8$) appeared as an X-ray diffraction artefact and transmission electron microscopy confirmed that the $Ba_8Zn_xGe_{46-x-y}[\ ]_y$ effectively crystallize within the clathrate type I structure.

The electron density ([n]) varies in quantitative agreement with the Zintl rules for y = 0 while for $y \neq 0$, [n] breaks the Zintl rules. $Ba_8Zn_8Ge_{38}$ displays the best thermoelectric properties (ZT = 0.07 at 300K) in this series.

Introduction

Type I clathrates $A_8M_xGe_{46-x}[\ ]_y$ (M = VIII, IB, IIB or IIIA elements, [ ] = Ge-vacancy) are constituted by large 20- and 24-atom cages filled by electropositive group IIA elements (A). The M = Ga and A = Sr, Ba, Eu compounds attracted great interest because they display ZT values larger than 1 at 800-900K [1-4]. They belong to the "Phonon Glass and Electron Crystal" class of materials since the quasi localized vibrations of the electropositive A- element in the 20- and 24-atom cages are thought to strongly reduce the lattice thermal conductivity to values as low as 1 $W.m^{-1}.K^{-1}$ [1]. Band structure calculations in $A_8Ga_{16}Ge_{30}$ (A = Sr, Ba, Eu) confirmed that these compounds fulfil the Zintl rules: the eight A^{2+} atoms fully donate their 16 electrons to the gallium which behave as a 1-electron acceptor [5, 6]. However, the acceptor character of other M elements and of the vacancies has never been quantitatively adressed in details.

The $Ba_8Zn_xGe_{46-x-y}[\ ]_y$ ($4 \leq x \leq 8$) compounds were first reported by Kuhl et al [7] who speculated the relation y = 4-x/2 between the zinc and vacancies concentrations which implies complete charge compensation and semiconducting properties all along the series. This speculation seemed promising for the thermoelectric properties of the Zn-based clathates since the highest power factors (α^2/ρ) were found in Ga-based type I clathrates with formally complete charge compensation ($Ba_8Ga_{16}Ge_{30}$) [8]. We therefore decided to explore the unknown electronic transport properties of the $Ba_8Zn_xGe_{46-x-y}[\ ]_y$ series as a function of the compositional parameters x and y. During the course of this work, Melnychenko-Koblyuk et al. reported on the structural, thermal, phonon, and transport properties of the $Ba_8Zn_xGe_{46-x-y}[\ ]_y$ compounds [9]. There is an overall agreement between their results and ours but we explored in greater details the relation between composition and electron density. In our previous work [10], based on X-ray data, we reported a supertructure in these compounds. Here we present new X-ray data combined with transmission electron microscopy results which contradicts the earlier superstructure report and confirms that the $Ba_8Zn_xGe_{46-x-y}[\ ]_y$ compounds crystallize within the type I structure. We had also previously showed that Zn substitutes on the 6c site of the type I structure and that the vacancy fraction varies with the measured zinc concentration ([Zn]) like y = 3.3-0.54[Zn]. Here we report electron density measurements which help evaluating the electron acceptor character of both Zn and the Ge-vacancy.

Experimental

The $Ba_8Zn_xGe_{46-x-y}[\ ]_y$ (x = 2-8, y = 0-3) synthesis, X-ray powder diffraction measurements, Electron Probe Micro-Analyis (EPMA) and electronic transport coefficients measurements are described elsewhere [10].

A field emission microscope CM 200 FEG/ST-Lorentz (FEI Company) at an acceleration voltage of 200 kV was used for the high-resolution transmission electron microscopy (HR-TEM) experiments. The selected area electron diffraction (SAED) patterns were obtained in a FEI Tecnai 10 (LaB_6-source and 100 kV acceleration voltage).

Structure

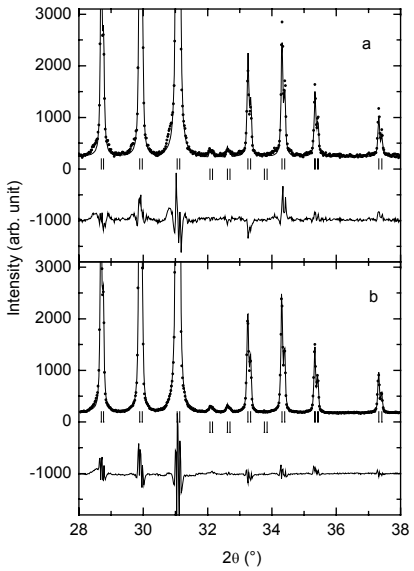

Figure 1. a- Experimental (circle) and calculated (line) diffraction pattern of $Ba_8Zn_8Ge_{38}$. Extra unindexed lines (left shoulders of the peaks) were initially attributed to a superstructure (see text. b- Second diffraction pattern of $Ba_8Zn_8Ge_{38}$ after changing the X-ray tube of the powder diffractometer used. $Ba_8Zn_8Ge_{38}$ can then be indexed within the clathrate type I structure.

The diffraction pattern of the $Ba_8Zn_xGe_{46-x-y}[\ ]_y$ samples ($2 \leq x \leq 8$) were successfully Rietveld-refined assuming a type I clathrate structure for the $Ba_8Zn_xGe_{46-x-y}[\ ]_y$ phase. We previously observed extra faint satellite lines in every diffraction pattern of the $Ba_8Zn_xGe_{46-x-y}[\ ]_y$ samples ($4 \leq x \leq 8$). It can easily be noticed in Fig. 1a that these extra lines (left shoulder of the main peaks) could not be indexed within the clathrate type I structure and were initially indexed within a *4a* x *4a* x *4a* supercell. This triggered a direct observation of the reciprocal lattice of these compounds by electron diffraction (SAED images) and by fast Fourier transform (FFT) of HR-TEM images. Every observed diffraction spots of the [101] (Fig. 2a), [122] (inset of Fig. 2b) [100], [112], [105] (not shown) zones could be indexed within the a = 10.763 Å cubic primitive lattice. Hence, no superstructure could be observed by SAED or HR-TEM. The apparent contradiction between the structure deduced from the first XRD and that obtained by HR-TEM was resolved by changing the X-ray tube of the X-ray diffractometer used in this study. Fig. 1b shows that no extra line can anymore be observed in the diffraction pattern of $Ba_8Zn_8Ge_{38}$. The extra faint lines (Fig. 3a) observed in every $Ba_8Zn_xGe_{46-x-y}[\ ]_y$ samples ($4 \leq x \leq 8$) were most likely arising from a double foyer effect of the former X-ray tube. It can therefore be concluded that the $Ba_8Zn_xGe_{46-x-y}[\ ]_y$ compounds ($4 \leq x \leq 8$) crystallize within the type I clathrate structure, in agreement with ref. [7, 9]. The results of the Rietveld refinements are summarized in Table I.

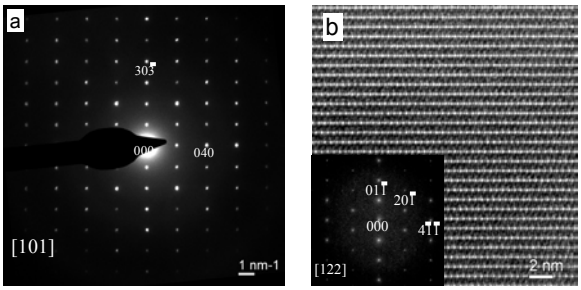

Figure 2. a- SAED pattern of $Ba_8Zn_8Ge_{38}$ along the [101] zone axis. b- HR-TEM image of $Ba_8Zn_8Ge_{38}$ along [122] direction. Neither the SAED pattern nor the fast Fourier transform (FFT) pattern (inset), show superlattice reflections.

Measured composition	*a* (Å)	V(Å^3)	x (16i)	y, z (24k)	R_p(%)
$Ba_{7.93}Zn_{7.53}Ge_{38.47}$ (B)	10.762	1246.46	0.185	0.312, 0.115	8.3
$Ba_{7.95}Zn_{7.1}Ge_{38.9}$	10.756	1244.38	0.184	0.310, 0.117	7.2
$Ba_8Zn_{6.29}Ge_{39.69}$	10.747	1241.26	0.184	0.313, 0.119	8.9
$Ba_8Zn_5Ge_{40.5}[\ ]_{0.5}$ *	10.736	1237.45	0.183	0.312, 0.119	9.3
$Ba_8Zn_{4.14}Ge_{40.73}$	10.715	1230.20	0.183	0.314, 0.120	9.3
$Ba_8Zn_{3.96}Ge_{41}$	10.710	1228.48	0.182	0.317, 0.120	10.2
$Ba_8Zn_{2.34}Ge_{41.54}$	10.688	1220.93	0.183	0.318, 0.120	8.1

Table I. EPMA measured composition, lattice parameter (*a*) of the type I clathrate, unit cell volume, coordinates of the 16i site (x, x, x) and of the 24k site (0, y, z) and reliability factor in the $Ba_8Zn_xGe_{46-x-y}[\ ]_y$ samples. * The composition of the x = 5 sample was not measured by EPMA and is nominal.

Electron density

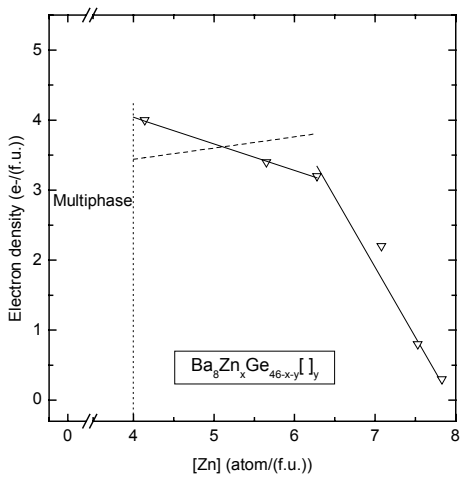

Figure 3. Experimental (triangle) and calculated (solid line) low temperature electron density ($[n_0]$) as a function of the measured Zn concentration [Zn]. For 4 ≤ [Zn] ≤6, the solid line corresponds to the linear fit $[n_0]$ = 5.6-0.38[Zn] to the data. The dashed line corresponds to a hypothetical electron density calculated from the Zintl rules [n] = 16 – 4*y-2[Zn] where the number of vacancies y = 3.3-0.54[Zn] is derived from the EPMA measurements and the Ge vacancies are assumed to be 4-electron acceptors. For [Zn] > 6, the solid line corresponds to $[n_0]$ = 2([Ba]-[Zn]) with [Ba] and [Zn] derived from EPMA.

Hall effect measurements were carried out in $Ba_8Zn_xGe_{46-x-y}[\ ]_y$ with x = 4-8 (the nearly single phase samples). In every sample, the measured Hall coefficients were negative implying that electrons are the majority charge carriers. The electron density ([n]) is weakly dependent on temperature over the interval [5-300K] and it ranges from 2.5 x 10^{20} to 3.3 x 10^{21} electron/cm^3. This is typical of "bad metals" or of semiconductors with a very large density of charge carriers, i.e. a highly degenerate semiconductor [11]. In order to compare with values derived from the Zintl rules, the low temperature electron density $[n_0]$ (e^-/(f.u.)) measured in $Ba_8Zn_xGe_{46-x-y}[\ ]_y$ is plotted in Fig. 3 as a function of the measured zinc concentration [Zn]. $[n_0]$ monotonously but not steadily decreases from 4.0 e^-/f.u. to 0.3 e^-/f.u with [Zn] increasing from 4 to 8. Two regimes can easily be observed in Fig.3 for the variations of $[n_0]$: weak decrease for 4≤[Zn]≤6 and a faster decrease when 6<[Zn]≤8. In the latter concentration range, there is no Ge vacancy and from the Zintl rules which assumes that Ba and Zn are respectively 2-electron donors and acceptors, the linear expression $[n_0]_{calc.}$ = 2[Ba]-2[Zn] can be derived (with [Ba] = 7.95). This calculated electron density is also plotted in Fig. 3 and it models very

well the measured $[n_0]$. Hence, when $6<[Zn]\leq 8$ this indicates that the free charge carrier properties of the $Ba_8Zn_xGe_{46-x}$ compounds fulfil the Zintl rules with Ba and Zn effectively acting as respectively 2-electron donor and acceptor. In the concentration range $4\leq[Zn]\leq 6$, the experimental data can be fitted linearly with the linear equation $[n_0] = 5.6-0.38[Zn]$. This does not correspond to the variations $[n_0] = 2[Ba]-4*y-2[Zn] = 2.8+0.16[Zn]$ (with $y = 3.3-0.54[Zn]$ derived from the EPMA measurements) which can be calculated from the assumption that the Ge vacancies are 4-electron acceptors (dashed line in figure 3). Assuming that Ba and Zn are respectively 2-electron donor and acceptor in the whole concentration range $4\leq[Zn]\leq 8$, the observed weak decrease of $[n_0]$ with [Zn] rather suggest that the vacancies can accept only less than 4 localized electrons. Identifying the fitted equation $[n_0] = 5.6-0.38[Zn]$ to the expression $[n_0] = 2[Ba]-Z_{vac}*y-2[Zn]$, with Z_{vac} the effective number of accepted electron per vacancy, $Z_{vac} = 3.0-3.2\ e^-$/vacancy is obtained. Hence the charge state of a Ge-vacancy would approximately be -3 in $Ba_8Zn_xGe_{46-x-y}[\ ]_y$ for $4\leq[Zn]\leq 6$. Qualitatively, a value larger than -4 for the charge state of the Ge vacancy can be understood as the result of electron-electron repulsions stronger than screening: this prevents the localization of 4 charges at the 6c site. Deeper understanding of this experimental result would of course require ab-initio electron density calculation.

Thermoelectric properties

As expected, the sample with the lowest electron density exhibits the largest power factor: $\alpha^2/\rho = 3.75\ \mu W.K^{-2}.cm^{-1}$ at 300K in $Ba_{7.95}Zn_{7.83}Ge_{38.17}$. Indeed, the compound with the largest measured zinc concentration (and closest to 8) is the best one, similarly to the $Ba_8Ga_xGe_{46-x-y}[\ ]_y$ series [8]. Assuming a thermal conductivity similar to $Ba_8Ga_{16}Ge_{30}$, ($\lambda = 1.5\ W.m^{-1}K^{-1}$), ZT = 0.07 at 300K in $Ba_8Zn_8Ge_{38}$. This value compares well with ZT = 0.09 at 300K published for polycrystalline $Ba_8Ga_{16}Ge_{30}$ by Kuznetsov et al. [12]. More transport measurements at high temperature are required to determine the potential for thermoelectric power generation of $Ba_8Zn_8Ge_{46}$.

References

[1] G. S. Nolas, et al., Appl. Phys. Lett. 73 (1998) 178.

[2] A. Saramat, et al., J. Appl. Phys. 99 (2006) 023708.

[3] H. Anno, et al., 21st International Conference on Thermoelectrics- Long Beach, California, USA - Aug. 25-29 (2002) 77.

[4] A. Bentien, et al., 22nd International Conference on Thermoelectrics ICT2003, La Grand Motte, France, August (2003) 131.

[5] N. P. Blake, et al., J. Chem. Phys. 114 (2001) 10063.

[6] G. K. H. Madsen, et al., Phys. Rev. B 68 (2003) 125212.

[7] B. Kuhl, et al., Z. Anorg. Allg. Chem. 621 (1995) 1.

[8] N. L. Okamoto, et al., J. Appl. Phys. 100 (2006) 073504.

[9] N. Melnychenko-Koblyuk, et al., J. Phys., Condens. Matter 19 (2007) 216223.

[10] E. Alleno, et al., 5th European Conference on Thermoelectrics, Odessa, Ukraine (2007) 108.

[11] H. Ibach, et al., *Solid State Physics* (Springer, Berlin, 1995).

[12] V. L. Kuznetsov, et al., J. Appl. Phys. 87 (2000) 7871.